Temperature statistics in two-dimensional stably stratified turbulence

Scott Wunsch*
Combustion Research Facility, Sandia National Laboratories, Livermore, California 94551-0969

Yuan-Nan Young
ASCI/FLASH Center at The University of Chicago, 5640 South Ellis Avenue, Chicago, Illinois 60637

(Received 4 March 2002; published 23 July 2002)

Using two-dimensional direct numerical simulations, the statistics of temperature differences in stably stratified turbulence are studied. Comparison with passive scalar statistics in similar flows suggests that the stably stratified case is qualitatively similar to the passive case. Probability distribution functions of temperature differences between points separated by different distances collapse using the same scalings in both passive scalar and stably stratified simulations. Some dependence on stratification strength is evident, but the qualitative similarity may be due to the dominance of the large-scale flow in determining the temperature statistics. We also explore the stratification dependence of the statistics of temperature values and gradients.

DOI: 10.1103/PhysRevE.66.016306 PACS number(s): 47.20.Bp, 47.27.−i

I. INTRODUCTION

The mixing of a passive scalar field in turbulent flows has been studied in great detail [1,2]. Recent work has suggested that large-scale anisotropies in the flow persist down to the smallest scales, and this has indicated a new kind of universal scaling in the statistics of large scalar differences [3]. This is possibly due to the existence of statistically conserved geometric objects in the flow [4,5], in which case the universal scaling may also apply to active scalars. Using two-dimensional numerical simulations, we find evidence that this universal scaling does extend to flows in which the scalar (temperature) is coupled to the turbulent dynamics by buoyant forces in a stably stratified flow. Such flows have relevance to many geophysical and astrophysical problems. In our simulations, a stable temperature gradient is imposed on the fluid, which is then stirred to generate turbulence. Using the Boussinesq approximation, the temperature field is coupled to the momentum equation by an imposed gravitational acceleration. In the absence of gravity this scenario reduces to the passive scalar case, while increasing the magnitude of the gravitational acceleration strengthens the coupling between the temperature field and the dynamics. This coupling influences the large-scale motions most strongly, determining a mixing length which is the major factor in the statistics of large fluctuations. We find that the tails of the probability density functions (PDFs) of temperature differences can be rescaled to obey a universal scaling which generalizes the form proposed in [3] to explicitly include the largest mixing length. The residual effect of the stratification on the dynamics is manifested only in minor changes to the shape of the rescaled PDF tails.

In addition to the statistics of temperature differences, we also study the statistics of temperature values and temperature gradients. Again, we find that the largest mixing length plays a central role in determining the rare events of these quantities.

*Corresponding author. Email address : sewunsc@sandia.gov

II. PROBLEM DESCRIPTION

To examine the statistics of the temperature field we employ two-dimensional simulations analogous to those described by Celani *et al.* [3] and Boffetta *et al.* [6] for the passive scalar case. As in [6], we define the velocity field using the stream function $\psi(\mathbf{x},t)$, from which the velocity components $u=\partial_z\psi$ and $w=-\partial_x\psi$ are derived. In addition, the temperature field $T(\mathbf{x},t)$ evolves with the flow and couples to the fluid density via the buoyancy term in the momentum equation. In the Boussinesq limit, the two-dimensional Navier-Stokes equations are expressed in terms of the vorticity $\omega(\mathbf{x},t)=\nabla^2\psi$ and ψ as

$$\partial_t\omega + J = \nu_n\nabla^{2n}\omega - \lambda\omega - \nabla^2 f - g\alpha\partial_x T, \tag{1}$$

where $J\equiv\partial_z\psi\partial_x\omega-\partial_x\psi\partial_z\omega$ is the usual Jacobian, f is a forcing function which adds energy to the flow at small scales, $\lambda\omega$ is a friction term which dissipates energy at large-scales, g is the gravitational acceleration, and α is the volume expansion coefficient of the fluid. The temperature is passive if the coupling $g\alpha$ is zero. The friction term $(\lambda\omega)$ dissipates energy at some characteristic wave number k_d in the passive scalar case. This friction term is equivalent to one proposed by Paret and Tabeling [7,8] to parametrize the large-scale dissipation in their magnetically driven two-dimensional turbulence experiments. A linear friction term also arises in two-dimensional magnetohydrodynamic turbulence [9], in which case λ represents a particle collision frequency. The forcing function f is a small-scale random source with amplitude f_0 which generates velocity fluctuations with a characteristic wave number k_f. As in [3] and [6], the usual Laplacian term for the viscous dissipation is replaced by an eighth order $(n=4)$ hyperviscosity, adjusted so as to be negligible except on scales smaller than the forcing scale. This use of hyperviscosity to improve numerical efficiency is a standard practice, and since the velocity forcing already introduces a degree of artificiality on the smallest scales, it may not be any less physical than normal viscosity. However, these details should be of minor consequence in this

work since our attention is focused on length scales larger than the energy injection scale.

The temperature field is advected according to the usual equation:

$$\partial_t T + \vec{u} \cdot \vec{\nabla} T = \kappa \nabla^2 T. \tag{2}$$

The diffusivity κ is chosen so that temperature fluctuations are dissipated at a scale slightly larger than the forcing scale k_f. An average temperature gradient g_0 aligned with the gravitational acceleration is imposed by means of jump-periodic boundary conditions, and temperature fluctuations $\theta \equiv T - g_0 z$ are then defined as deviations from the imposed gradient. The velocity boundary conditions are periodic.

The numerical resolution for all the results in this paper is 2048×2048 and the statistics are collected over 10–25 large-eddy turnover times in each of our simulations. For the passive case the friction coefficient λ is chosen so that the dissipation scale is approximately 1/3 of the box size. For nonzero $g\alpha$, the dissipation scale decreases from its passive scalar value.

In stably stratified turbulent shear flow, the influence of the stratification on the dynamics is characterized by the Richardson number $\mathrm{Ri} \equiv g\alpha g_0 \Lambda^2 / U_\Lambda^2$, which gives the ratio of potential to kinetic energy on the length scale Λ. We apply the same definition to our two-dimensional simulations, with $\Lambda \equiv 2\pi/k_d$ being the energy dissipation scale and the integral scale velocity being $U_\Lambda \equiv \sqrt{\langle w^2 \rangle}$. We use the vertical velocity component to define U_Λ because this is the component that transports fluid along the temperature gradient. Because the energy input occurs at the small scales in our simulations, it is also useful to define a forcing-scale Richardson number Ri_f given by $\mathrm{Ri}_f \equiv g\alpha g_0 / f_0 k_f^2$. It indicates the ratio of potential to kinetic energy on the forcing scale k_f^{-1}. In our work, Ri_f is an input parameter defining the dimensionless stratification strength while Ri must be computed from the observed dissipation scale quantities Λ and U_Λ. As Ri_f is increased, the integral scale Richardson number Ri also increases while the integral scale Λ decreases.

As described in [6], the two-dimensional Navier-Stokes equations produce an inverse kinetic energy cascade with a $k^{-5/3}$ power spectrum within an ''inertial range'' bounded by the large dissipation scale k_d^{-1} and the small forcing scale k_f^{-1}. Figure 1 shows kinetic energy spectra $E(k)$ for three of the simulations, compensated by the expected scaling of $k^{-5/3}$. As Ri increases, the inertial range [in which $E(k)k^{5/3}$ is approximately constant] shortens due to the influence of the stratifcation on the largest scales (decreasing Λ). In the inertial range the kinetic energy at any given length scale increases slightly with the Richardson number [i.e., $E(k)k^{5/3}$ increases slightly with Ri]. However, the principal dynamical effect of the stratification is the decrease in the integral scale Λ as Ri increases. There is also a slight asymmetry in the velocity component magnitudes which increases with Richardson number, with ($\sqrt{\langle u^2 \rangle}$) being approximately 30% larger than ($\sqrt{\langle w^2 \rangle}$) in the highest Ri case.

While a precise determination of k_d from the spectra is not possible, we estimate k_d from the wave number where $E(k)k^{5/3}$ first reaches 1/10 of its inertial range value. These estimates are consistent with

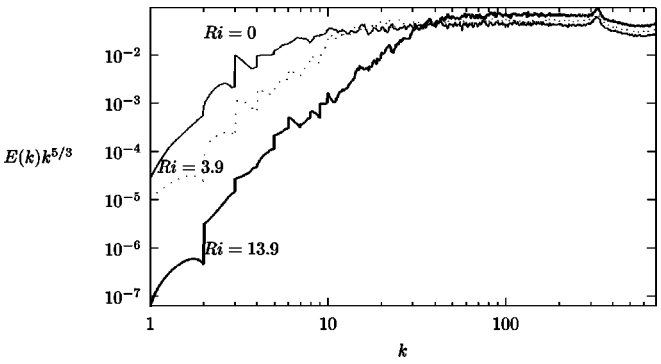

FIG. 1. Velocity spectra for three different Richardson numbers. Energy is injected at $k_f \sim 330$ and cascades to lower wave numbers until reaching the integral scale (which depends strongly on Ri).

$$\Lambda(\mathrm{Ri}_f) = \frac{\Lambda(0)}{1 + 4546 \mathrm{Ri}_f^{0.67}}. \tag{3}$$

We use the estimate of Λ given by Eq. (3) to rescale our PDFs from different Richardson number simulations and demonstrate a universal scaling. In our simulations $\Lambda(\mathrm{Ri}_f)$ varies by a factor of approximately 6. The dynamical impact of the stratification is therefore quite significant. Although the velocity spectra are slightly anisotropic due to the asymmetric effects of the buoyancy term, estimates of Λ from individual velocity component spectra differ from the estimate of Eq. (3) by only a few percent at most. The precise values of the input parameters (Ri_f) and computed quantities (Ri, Λ, etc.) for the six simulations presented here are summarized in Table I.

In this paper we focus on the role of the integral scale Λ in the temperature statistics. The influence of Λ is expected to be strongest when one considers temperature values that deviate substantially from the mean gradient. This is because the fluid elements involved must have been transported a large distance to achieve a large deviation. However, the length scale Λ does not play a major role in determining the statistics of the high probability, small-deviation events (the core of the PDF).

III. STATISTICS OF TEMPERATURE DIFFERENCES

We first consider the statistics of the two-point temperature difference, defined as $\delta\theta(\mathbf{r}) \equiv \theta(\mathbf{x}+\mathbf{r}) - \theta(\mathbf{x})$. The PDF

TABLE I. Quantities for the simulations with a domain size of 2π and a forcing wavelength of $k_f \sim 330$.

$\mathrm{Ri}_f \times 10^6$	0	0.405	1.22	4.05	12.2	40.5
Ri	0.0	0.9	2.2	3.9	8.1	13.9
$\sqrt{\langle \theta^2 \rangle}$	0.24	0.21	0.11	0.049	0.019	0.0056
$\sqrt{\langle u^2 \rangle}$	0.63	0.63	0.59	0.53	0.45	0.37
$\sqrt{\langle w^2 \rangle}$	0.60	0.55	0.51	0.44	0.36	0.28
Λ	2.10	1.68	1.42	0.90	0.60	0.34

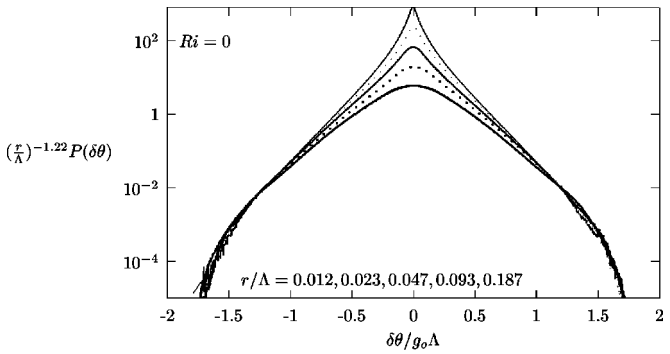

FIG. 2. Scaling of the PDF of temperature differences at pairs of points separated by five different distances r (in any direction) in the inertial range of Ri$=0$. The tails (but not the cores) collapse to the same form.

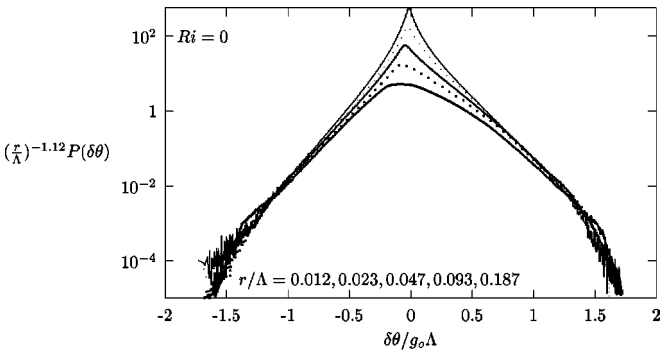

FIG. 3. Scaling of the PDF of temperature differences at pairs of points separated by five different distances r (in the vertical direction only) in the inertial range Ri$=0$. The tails (but not the cores) collapse to the same form.

of $\delta\theta$ quantifies the likelihood of observing a "jump" in the temperature of $\delta\theta$ between two points separated by a distance **r**. While little is known experimentally about the full PDF of $\delta\theta$, its moments [known as structure functions, $S_{2n}(r) \equiv \langle \delta\theta^{2n}(r) \rangle$ for moment $2n$] have been observed to scale with the separation r with exponents ζ_{2n} which are nonlinear functions of n [10–12]. Based on two-dimensional simulations similar to ours, it was suggested by Celani *et al.* [3] that these exponents approach a constant value ζ in the limit $n \to \infty$ due to an underlying PDF with tails of the form

$$p(\delta\theta(r)) \sim \left(\frac{r}{\Lambda}\right)^{\zeta} Q\left(\frac{\delta\theta}{g_0\Lambda}\right), \tag{4}$$

where $Q(\delta\theta/g_0\Lambda)$ is some universal function. The nondimensionalization with the integral scale Λ is introduced here to expedite comparisons between PDFs from simulations with different stratification strengths (and hence different Λ's). This is a generalization from [3], in which temperature differences were scaled with θ_{rms}, but this change is of no consequence when comparing PDFs for different r within the same simulation (same Λ and θ_{rms}). The form of Eq. (4), utilizing Λ, is based on the assumption that the largest mixing length is the dominant factor in determining the rare event statistics. The significance of the largest mixing length was previously suggested in a simple stochastic mixing model, in which $Q(\delta\theta) \sim \exp(-C|\delta\theta|)$ and the constant C was shown to scale as $(g_0\Lambda)^{-1}$ [13]. The approach of the structure function scaling exponents ζ_{2n} to a constant was observed in the simple model as well.

Due to the directional asymmetry of the flow, we studied PDFs of temperature differences $\delta\theta$ between points separated by a distance r in the horizontal and vertical directions, as well as PDFs constructed from separations in all directions. Similar qualitative conclusions apply to all cases, but the quantitative details are directionally dependent. Figures 2 and 3 present PDFs of $\delta\theta$ from the passive scalar simulation (Ri$=0$) for all directions and for vertical separations only, respectively. Horizontal separation PDFs are omitted for brevity. Both PDFs are presented in the form of Eq. (4), showing the collapse of the tails for different values of the separation r. The exponent ζ that produces the best collapse is directionally dependent, with $\zeta = 1.28$ collapsing the horizontal separation PDFs, $\zeta = 1.12$ collapsing the vertical separation PDFs, and $\zeta = 1.22$ collapsing PDFs constructed using all separation directions. Our error estimate for the exponents is approximately ± 0.06. The collapse is demonstrated for five inertial range separations from just larger than the forcing scale to approximately 1/5 of the integral scale Λ, a factor of 16. The tails collapse for $|\delta\theta| \geqslant g_0\Lambda$, suggesting that the universal form applies to events in which fluid elements initially separated by at least one integral scale (and hence differing in temperature by at least $g_0\Lambda$) are transported to close proximity before equilibrating with their new environments. The long transport distance required to achieve the temperature differences that obey Eq. (4) supports the assumption that it is the large-scale motions which are primarily responsible for the collapse of the PDF tails.

Figures 4 and 5 demonstrate the same collapse of the PDFs of temperature differences $\delta\theta$ in a strongly stratified simulation (Ri$=8.1$). The exponents ζ required for the collapse are the same as in the passive scalar case. Due to the smaller integral scale Λ, only four values of r, up to 1/3 of the integral scale separation (eight times the smallest separation), are shown in this case. The PDFs from all six simulations described in Table I collapsed when rescaled using the same numerical exponents as in the passive scalar case.

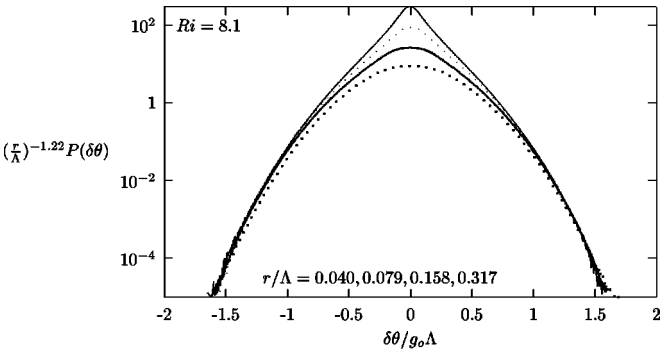

FIG. 4. Scaling of the PDF of temperature differences at pairs of points separated by four different distances r (in any direction) in the inertial range for Ri$=8.1$. The tails (but not the cores) collapse to the same form.

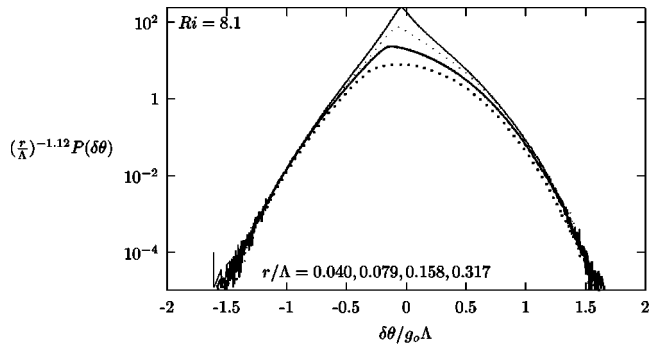

FIG. 5. Scaling of the PDF of temperature differences at pairs of points separated by four different distances r (in the vertical direction only) in the inertial range Ri=8.1. The tails (but not the cores) collapse to the same form.

These values of ζ reported here differ from the value $\zeta=1.4$ reported in [3]. However, the value of ζ may depend on many factors, as suggested by a recent numerical study of thermal plume turbulence in which $\zeta=0.8$ [14]. The important fact is that the same value of ζ works for all stratification strengths (all Ri) in our simulations.

It has been shown that the tails of the PDFs are of the form of Eq. (4) for both zero and nonzero stratification strengths. Although the scalings with r/Λ appear to be identical in both cases, this does not imply that the function $Q(\delta\theta/g_0\Lambda)$ is necessarily independent of Ri. Figure 6 shows this function for four different Ri at the same value of r/Λ for all separation directions, and Figure 7 shows the Q for vertical separations only. The nonzero Ri Q's appear to converge to a single shape function, while the passive scalar (Ri=0) case has a distinct Q. Hence, when different nonzero stratification strengths are compared (such that Λ is significantly smaller than its passive scalar value), the value of Λ appears to completely control the PDF scaling, since Q becomes independent of Ri. It is worth emphasizing that this collapse of the PDFs for different Ri does not occur if the original form of Eq. (4) proposed in [3] (using θ_{rms} rather than Λ) is used. It is not surprising that the passive and stratified cases have a different shape function Q, since the large-scale dynamics are controlled by the λ dissipation term

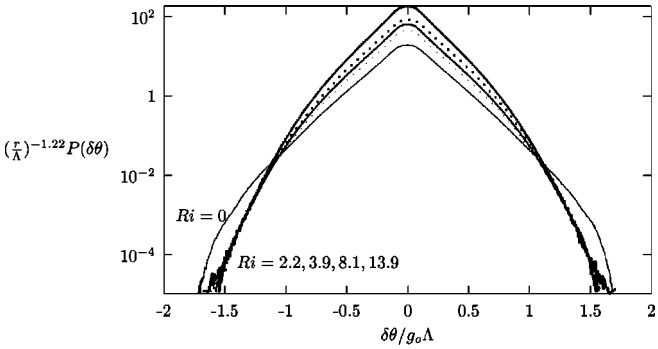

FIG. 6. Comparision of the shape function Q for different Richardson numbers for an inertial range separation $r\simeq0.08\Lambda$ (in any direction). The shape function Q for the passive scalar case is distinct from the stably stratified cases, which collapse.

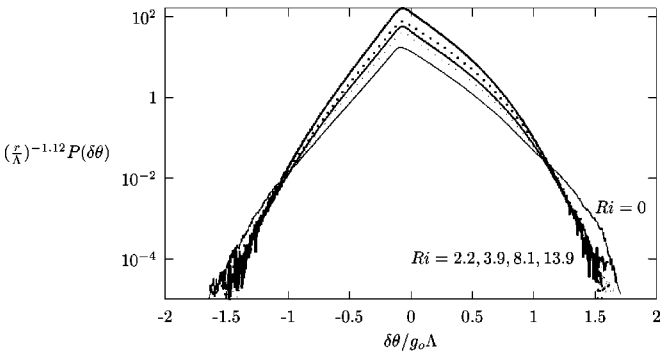

FIG. 7. Comparison of the shape function Q for different Richardson numbers for an inertial range separation $r\simeq0.08\Lambda$ (in the vertical direction only). The shape function Q for the passive scalar case is distinct from the stably stratified cases, which collapse.

in the former case but by the $g\alpha$ coupling term in the latter case. However, since $g_0\Lambda$ varies by a factor of 6 between the passive scalar case and the largest-Ri case, the tails of the actual PDFs $P(\delta\theta)$ differ by many orders of magnitude at any specific value of $\delta\theta$, while the reduced shape functions Q differ by less than one order of magnitude. The large mixing length Λ is therefore the principal factor in determining the PDF, with differences in the detailed dynamics of the passive and stratified simulations playing a secondary role as reflected in the distinct shape functions Q.

Since the structure functions $S_{2n}(r)$ are the moments of the PDFs, they should scale as

$$S_{2n}(r)\sim(g_0\Lambda)^{2n}\left(\frac{r}{\Lambda}\right)^{\zeta} \tag{5}$$

in the limit $n\to\infty$ if Eq. (4) is a good description of the tails of the PDF. Figure 8 shows structure functions for separation increments in all directions from the Ri=0 simulation. The straight lines on the log-log plot in the inertial range indicate scaling behavior. Similar results were observed in the nonzero Richardson number simulations (with shorter scaling ranges). Actual scaling exponents for three different Richardson number cases are shown in Fig. 9. The exponent ζ_2 of the secord order structure function has the expected value of 2/3 in the Ri=0 case. In all Ri cases the exponents approach a constant value for large n which is consistent with the exponent 1.22 that best collapses the PDF tails. The scaling

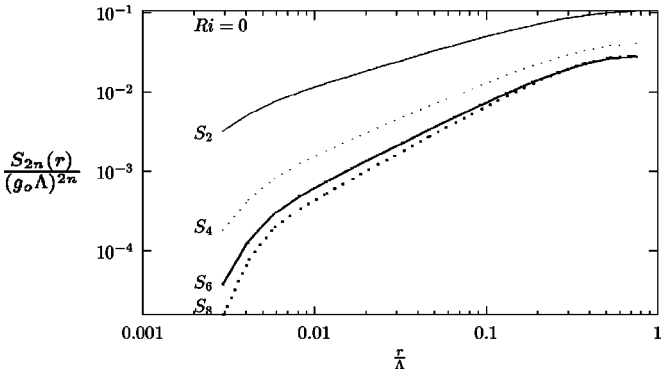

FIG. 8. Structure functions for the passive scalar (Ri=0) case.

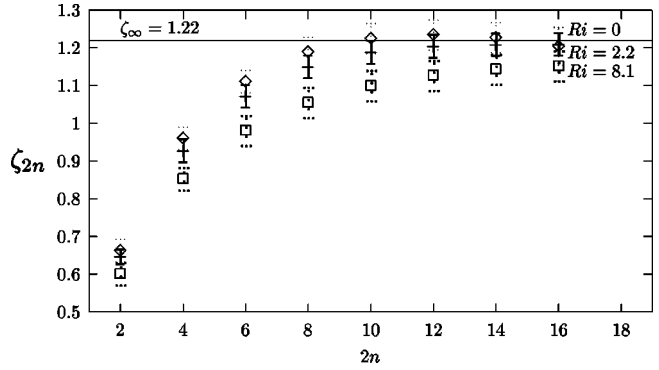

FIG. 9. Structure function scaling exponents for three different Richardson numbers. The exponents appear to approach a constant in the limit $n \to \infty$. The exponents are consistent with the limit $\zeta_\infty = 1.22$ inferred from the PDF collapse.

exponent of any finite moment structure function depends on the PDF core as well as the tails, and hence can take a value that depends on Ri despite the universal scaling of the tails.

Thus far the importance of the integral scale Λ in determining the statistics of large temperature deviations has been demonstrated. One would not expect Λ to play a crucial role in the statistics of small temperature deviations (the PDF core), since the generation of small temperature deviations does not require transport across great distances. The scaling of Eq. (4) applies only to the tails and does not collapse the core of the two-point PDFs. A possible scaling for the core was recently suggested in [14]:

$$p(\delta\theta(r)) \sim \left(\frac{r}{\Lambda}\right)^{-\alpha} F\left(\frac{\delta\theta}{g_0\Lambda}\left(\frac{\Lambda}{r}\right)^{\alpha}\right). \tag{6}$$

Again, we have normalized the separations r and temperature differences $\delta\theta$ using the integral scale Λ, as in Eq. (4). This scaling appears to apply only to horizontal separations in the passive scalar case, with $\alpha = 0.55$. Due to the asymmmetry of the PDFs constructed using vertical separations at all Ri (see Figs. 3 and 5, for example), the vertical PDFs do not collapse, as the degree of asymmetry varies with r. We also find that the collapse fails in all stably stratified cases, even when restricted to horizontal separations. These results suggest that the PDF cores depend sensitively on the details of the dynamics at all length scales, rather than being governed primarily by the value of the integral scale Λ. This is not surprising, since small temperature differences can be generated by motions much smaller than Λ.

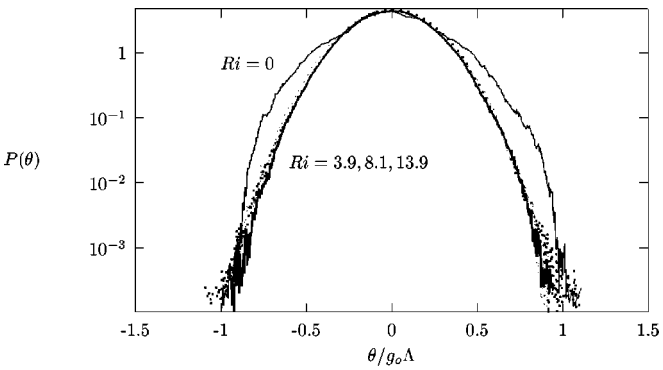

FIG. 10. Rescaled PDFs of temperature values θ, illustrating the collapse of the nonzero Ri PDFs.

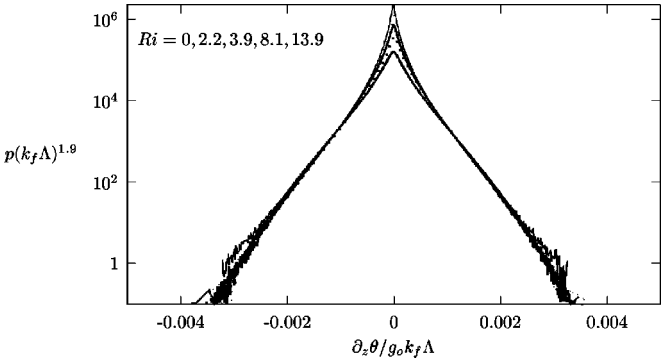

FIG. 11. Rescaled PDFs of horizontal temperature gradients.

IV. OTHER STATISTICAL MEASURES

The simplest statistical quantity examined in passive scalar flow is the fluctuation of the temperature from the mean gradient, $\theta(\mathbf{x})$. While it has been observed experimentally that the probability distribution function $p(\theta)$ exhibits exponential tails, i.e., $p(\theta) \sim \exp(-|\theta| g_0\Lambda)$ for $|\theta| \gg g_0\Lambda$, in both grid turbulence [15,16] and pipe flow [17] experiments, we do not see clear evidence of this in our simulations. Figure 10 shows PDFs of θ from our simulations at four different stratification strengths. The PDFs are normalized by $g_0\Lambda$, and two distinct shapes—one for the passive scalar and one for strong stratification—are evident. The collapse of the PDFs in the limit of strong stratification is an indication that the largest mixing length Λ is the major factor in determining the statistics of large temperature fluctuations as well as temperature differences.

In the limit of zero separation ($r \to 0$), temperature differences $\delta\theta(r)$ reduce to temperature gradients. The PDFs of temperature gradients, $\partial_x\theta$ and $\partial_z\theta$, have been observed to have exponential tails in stably stratified grid turbulence experiments [18]. Searching for a universal form for the PDFs of temperature gradients, we consider equation 4 in the limit of small separations r, such that $\delta\theta(r) \simeq r\partial_x\theta$. However, since Eq. (4) only applies to inertial range separations, we

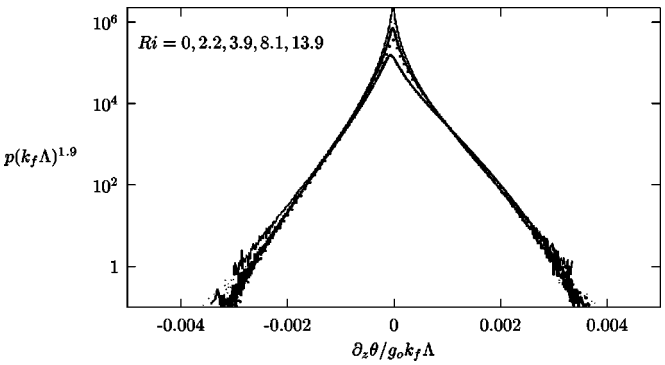

FIG. 12. Rescaled PDFs of vertical temperature gradients.

guess that at separations smaller than the minimum inertial separation $r \sim k_f^{-1}$ the PDFs will no longer scale with r but rather retain the form of the $r \sim k_f^{-1}$ PDF. This leads us to assume the scaling

$$p(\partial_x \theta) \sim \left(\frac{1}{k_f \Lambda} \right)^{\beta} Q' \left(\frac{\partial_x \theta}{k_f g_0 \Lambda} \right) \tag{7}$$

for the PDF of temperature gradients (which applies to $p(\partial_z \theta)$ for vertical separations as well). This expresses the expected dependence of the gradient PDFs on the stratification strength through Λ. Figures 11 and 12 show the horizontal and vertical temperature gradient PDFs in the form of Eq. (7) for five different Richardson numbers. The exponent $\beta = 1.9$ was fitted from the three largest Ri simulations, which collapse perfectly, with Q' taking the form of an exponential (as in the experiments). The passive scalar and low-Ri simulations do not match perfectly but the differences are small. As with inertial range separations, it appears that the large length scale Λ dominates the statistics of rare events even at small scales, but that passive scalar and strongly stratified flows are slightly different in their details. Again, the different dynamics at the largest length scale (controlled by the friction term in the passive case, but by buoyancy in the stratified case) may be the source of the distinction.

V. CONCLUSIONS

The simulations presented here suggest that the statistics of large temperature differences in stably stratified flows obey a universal scaling determined by the separation between the points. This extends the scaling suggested by Celani *et al.*, [3] for the passive scalar case to the active scalar regime. Using an integral scale determined from the velocity spectra, PDF tails from a range of nonzero stratification strengths were shown to have identical shapes when rescaled, although this shape differed slightly from the shape of the rescaled passive scalar PDF tails. This distinction may be attributed to the different large-scale dynamics in the passive scalar case, which are due to the friction term used. The convergence of the rescaled PDFs in the stably stratified simulations indicate that the largest mixing length (integral scale) is the dominant factor in determining the statistics of large temperature differences, and that the generalized scaling of the PDFs suggested here may be used to compare statistics between flows with different integral scales.

Similarly, the integral scale was also shown to be a major factor in the rare event statistics for temperature values and temperature gradients, as indicated by the collapse of the tails of the rescaled PDFs of these quantities. As with temperature differences, a slight distinction was observed between passive scalar and strongly stratified flows, reflecting the residual effects of the different dynamics in the two cases after accounting for the consequences of the variation in integral scale.

ACKNOWLEDGMENTS

It is a pleasure to acknowledge helpful conversations with Alan Kerstein and Bob Rosner. This work was supported by the Division of Chemical Sciences, Office of Basic Energy Sciences, U.S. Department of Energy, and by the ASCI Flash Center. The authors also thank the Argonne National Lab and Sandia National Laboratories for providing computing resources. Y.N.Y. acknowledges support from NASA and Northwestern University.

[1] Z. Warhaft, Annu. Rev. Fluid Mech. **32**, 203 (2000).
[2] B. Shraiman and E. Siggia, Nature (London) **405**, 639 (2000).
[3] A. Celani, A. Lanotte, A. Mazzino, and M. Vergassola, Phys. Rev. Lett. **84**, 2385 (2000).
[4] A. Celani and M. Vergassola, Phys. Rev. Lett. **86**, 424 (2001).
[5] I. Arad, L. Biferale, A. Celani, I. Procaccia, and M. Vergassola, Phys. Rev. Lett. **87**, 164502 (2001).
[6] G. Boffetta, A. Celani, and M. Vergassola, Phys. Rev. E **61**, R29 (2000).
[7] J. Paret and P. Tabeling, Phys. Rev. Lett. **79**, 4162 (1997).
[8] J. Paret and P. Tabeling, Phys. Fluids **10**, 3126 (1998).
[9] D. Biskamp and E. Schwarz, Europhys. Lett. **40**, 637 (1997).
[10] R.A. Antonia, E.J. Hopfinger, Y. Gagne, and F. Anselmet, Phys. Rev. A **30**, 2704 (1984).
[11] L. Mydlarski and Z. Warhaft, J. Fluid Mech. **358**, 135 (1998).
[12] F. Moisy, H. Willaime, J. Anderson, and P. Tabeling, Phys. Rev. Lett. **86**, 4827 (2001).
[13] S. Wunsch, Phys. Rev. E **58**, 5757 (1998).
[14] A. Celani, A. Mazzino, and M. Vergassola, Phys. Fluids **13**, 2133 (2001).
[15] J.P. Gollub, J. Clarke, M. Gharib, B. Lane, and O.N. Mesquita, Phys. Rev. Lett. **67**, 3507 (1991).
[16] Jayesh and Z. Warhaft, Phys. Rev. Lett. **67**, 3503 (1991).
[17] J.E. Guilkey, A.R. Kerstein, P.A. McMurtry, and J.C. Klewicki, Phys. Rev. E **56**, 1753 (1997).
[18] S.T. Thoroddsen and C.W.V. Atta, J. Fluid Mech. **244**, 547 (1992).